ARCHIVES OF CIVIL ENGINEERING, LVI, 2, 2010

DOI: 10.2478/v.10169-010-0007-8

QUASI-STATIC FAILURE CRITERIA FOR CONCRETE

T. JANKOWIAK[1], T. ŁODYGOWSKI[2]

The behaviour of concrete under quasi-static loadings for uniaxial compression, tension and plane stress conditions is studied. The failure criteria of concrete are discussed as well as the methods of constitutive parameters identification are elaborated. The attention is focus on an energetic interpretation of selected failure criteria. The numerical example with concrete damage plasticity material model is shown.

Key words: concrete strength, constitutive parameters, identification, energetic interpretation.

1. Introduction

Numerical methods are essential elements in design process of structure, particularly for unique loadings. To predict real behaviour of a structure subjected to unique loadings, the using of a failure criterion for concrete is required. The unique loadings are destructive for whole structure (load capacity decreasing) or for parts of structure (damage).

The proper description of concrete strength in an advance state of stress is crucial for future computations. This strength should not be described basing only on simple tests as tension, compression and shear [5, 15]. Typical concrete for which compressive strength is f_c, in the case of additional shear on the level of $0.08\ f_c$, fails with compressive strength equals only $0.5 f_c$. Therefore the concrete strength should be described through taking into consideration mutual interaction of different components of a stress state. In this paper, the presentation of quasi-static failure criteria for concrete as a function of stress state for three-dimensional cases is included. In the past, several failure criteria were presented [2, 5, 15, 17, 21] and some of them are also chosen and discussed in this work. Additional, the interpretation in energetic spaces of the most often used criteria is shown. In the case of a concrete in three-dimensional state of stress, we observe a number of criteria, plastic flow criterion and initiation of cracking

[1] Institute of Structural Engineering (ISE), Poznan University of Technology, Piotrowo 5, 60-965 Poznań, Poland, e-mail: tomasz.jankowiak@put.poznan.pl

[2] Institute of Structural Engineering (ISE), Poznan University of Technology, Piotrowo 5, 60-965 Poznań, Poland, e-mail: tomasz.lodygowski@put.poznan.pl

or strength criteria. During the final stage of deformation, together with the increasing of deformations, the failure is detected.

In principle, the concrete failure is divided into two types. First it appears by dominant tension and second by dominant compression [4]. Failure in tension is connected with appearing of the crack and generally with decreasing of the capacity in the direction perpendicular to the principal tension direction. In compression, it approaches to initiation and evolution of number of micro-cracks. The crushing of concrete is reached. It is connected with decreasing of the capacity of concrete.

2. Properties of concrete for quasi-static loadings

The compression test of a concrete in general predicts the quality of concrete and carries the qualitative information on its internal micro-structure. The real tensile strength is smaller than the theoretical one, what is computed based on molecular cohesion and surface energy of the perfect homogenous body. This strength reaches [19] and mainly depends on the cohesion of aggregates and hardened cement paste. Fig. 1 presents the failure surfaces under the plane stress conditions for different classes of concretes based on laboratory tests [16].

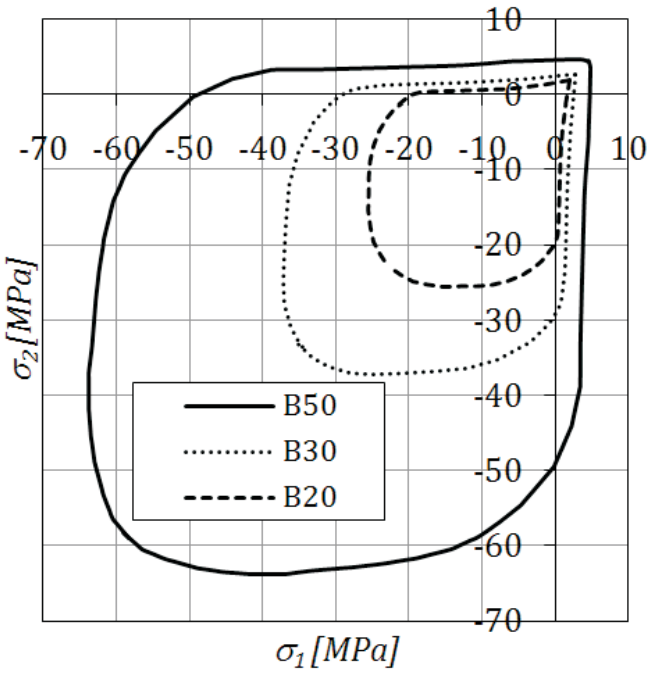

Fig. 1. Kupfer's curves for different class of concrete.
Rys. 1. Krzywe Kupfera dla różnych klas betonu

3. Failure criteria

The failure criteria for quasi-static loading cases can be expressed in the following form:

$$f(I_1, J_2, J_3) = 0, \tag{3.1}$$

where I_1 is first invariant of stress tensor σ_{ij}, J_2 end J_3 are the second and the third invariant of stress deviator s_{ij}, respectively. The whole elastic energy density over the volume material unit W can be divided into two parts [8]. The first W_1 is connected with the change of volume, while the second one W_2 with the change of a shape according to $W = W_1 + W_2$, where:

$$W_1 = \frac{1-2v}{6E} I_1^2, \tag{3.2}$$

$$W_2 = \frac{1+v}{E} J_2. \tag{3.3}$$

E and v are Young modus and Poisson ratio. Invariants I_1, J_2 are directly connected with the strain energy density of volume change W_1 and with strain energy density of distortion W_2, respectively.

3.1. The Burzyński (B) energetic failure criterion

The hypothesis assumes that failure is conducted by the strain energy density of distortion as in Huber-Mises condition increased by a part of volume change strain energy density [3]. Mathematical form of this assumption is expressed by the following equation:

$$\phi_f + \eta\phi_v = K, \tag{3.4}$$

where

$$\begin{aligned} \phi_f &= W_2 = \frac{1+v}{E} J_2, \\ \phi_v &= W_1 = \frac{1-2v}{6E} I_1^2, \end{aligned} \tag{3.5}$$

are the strain energies density of distortion and of volume change, respectively. The last element is a function η, which is the matching function of the first invariant of stress tensor and accordingly to the proposed by Burzyński form is:

$$\eta = \eta(W_1) = \omega + \frac{\delta}{3p} = \omega + \frac{\delta}{I_1} = \omega + \frac{\delta}{\pm\sqrt{\frac{6E}{1-2v}W_1}}, \tag{3.6}$$

where hydrostatic pressure is:

$$p = \frac{I_1}{3} \tag{3.7}$$

The Eq. (3.4) after taking into consideration dependences Eqs (3.5)-(3.6) has the form:

$$W_2 = K - \omega W_1 \mp \delta\sqrt{\frac{1-2v}{6E}}W_1. \tag{3.8}$$

The sign „+" is applied to the situation if $I_1 \geq 0$ and „–" if $I_1 < 0$. Three constitutive parameters ω, δ and K are identified by the three laboratory tests: uniaxial compression $(-f_c, 0, 0)$ and tension $(f_t, 0, 0)$ and biaxial uniform compression $(-f_bc, -f_bc, 0)$. In Tab. 1 are the all necessary data, which are required to the created system of equations:

$$\begin{cases} \frac{1+v}{E}\frac{f_t^2}{3} = K - \omega\frac{1-2v}{6E}f_t^2 + \delta\sqrt{\left(\frac{1-2v}{6E}\right)^2 f_t^2} \\ \frac{1+v}{E}\frac{f_c^2}{3} = K - \omega\frac{1-2v}{6E}f_c^2 - \delta\sqrt{\left(\frac{1-2v}{6E}\right)^2 f_c^2} \\ \frac{1+v}{E}\frac{f_{bc}^2}{3} = K - \omega\frac{1-2v}{6E}4f_{bc}^2 - \delta\sqrt{\left(\frac{1-2v}{6E}\right)^2 4f_{bc}^2} \end{cases}. \tag{3.9}$$

By the solution of the system Eq. (3.9) we drive of three necessary parameters of failure surface. The fourth and the fifth columns in Tab. 1 are collected to construct the system of equation based on Eq. (3.8).

The solution of the system of Eq. (3.9) gives three constitutive parameters in the form:

$$\begin{cases} \omega = -\frac{1}{3}\frac{a\left(-f_{bc}^2 - 2f_tf_{bc} + f_tf_c + 2f_cf_{bc}\right)}{b\left(-4f_{bc}^2 + 2f_cf_{bc} - 2f_tf_{bc} + f_tf_c\right)} \\ \delta = -\frac{af_{bc}^2(f_c - f_t)}{b\left(-4f_{bc}^2 + 2f_cf_{bc} - 2f_tf_{bc} + f_tf_c\right)} \\ K = \frac{af_cf_tf_{bc}^2}{-4f_{bc}^2 + 2f_cf_{bc} - 2f_tf_{bc} + f_tf_c} \end{cases}, \tag{3.10}$$

Table 1

Data for identification of Burzyński criterion.
Dane do identyfikacji kryterium Burzyńskiego

Point	I_1	J_2	W_1	W_2
$(\sigma_1, \sigma_2, \sigma_3) = (f_t, 0, 0)$	f_t	$\frac{f_t^2}{3}$	$\frac{1-2v}{6E} f_t^2$	$\frac{1+v}{E} \frac{f_t^2}{3}$
$(\sigma_1, \sigma_2, \sigma_3) = (-f_c, 0, 0)$	$-f_c$	$\frac{f_c^2}{3}$	$\frac{1-2v}{6E} f_c^2$	$\frac{1+v}{E} \frac{f_c^2}{3}$
$(\sigma_1, \sigma_2, \sigma_3) = (-f_b c, -f_b c, 0)$	$-2f_b c$	$\frac{f_{bc}^2}{3}$	$\frac{1-2v}{6E} 4 f_{bc}^2$	$\frac{1+v}{E} \frac{f_{bc}^2}{3}$

where

$$a = \frac{1+v}{E}, b\frac{1-2v}{6E}. \tag{3.11}$$

For example assuming that $f_c = 30MPa$, $f_t = 3MPa$ and $f_{bc} = 33.6MPa$, the three constitutive parameters are obtained as $\omega = 1.1878, \delta = 140.069, K = 0.001556$.

The Burzyński energetic failure criterion [3, 20] in graphical form is presented in Fig. 2 (black continuous line). There are two visible lines, which considers invariant I_1 for opposite signs. The curve in Burzyński criterion passes through identification points and the strain energy of distortion W_2 from the specifed place (maximum) decreases together with increase of the volume change strain energy W_1. In addition, in Fig. 3 the shape of Burzyński failure surface under plane stress conditions is presented (black continuous line). Fig. 4 shows the shape of failure surface in meridian plane. The following function describes the shape in meridian plane:

$$r = \sqrt{\frac{2}{a}\left(K - 3b\omega\xi^2 - \sqrt{3}b\delta\xi\right)}. \tag{3.12}$$

It is important that Burzyński failure criterion reduces to other criteria. The possible cases are presented in original paper of Burzyński and discussed also later [12, 20].

3.2. OTHER FAILURE CRITERIA

Failure criteria are specific limit functions of stresses, strains or the invariants of stresses and strains. These functions can be used as the plastic potential functions or the loading functions to describe the inelastic deformation of concrete. It is possible

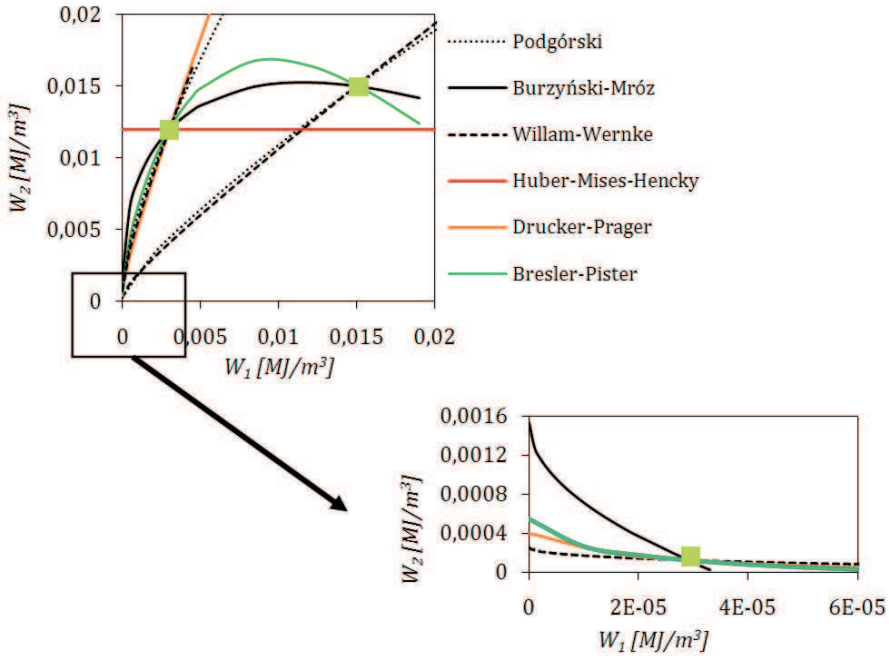

Fig. 2. Comparison of failure curves in space $W_1 - W_2$.
Rys. 2. Porównanie krzywych zniszczenia w przestrzeni $W_1 - W_2$

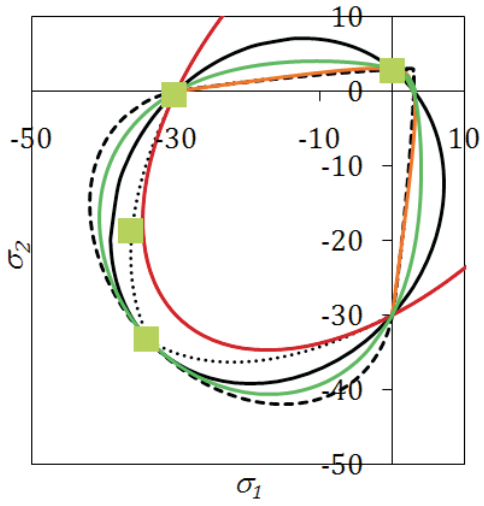

Fig. 3. Different failure criteria in plane stress conditions $\sigma_1 - \sigma_2$.
Rys. 3. Kryteria zniszczenia w płaskim stanie naprężenia $\sigma_1 - \sigma_2$

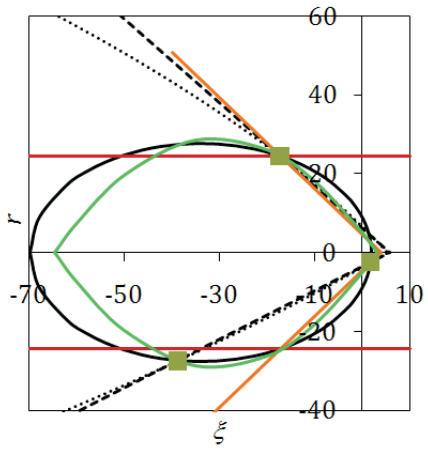

Fig. 4. Different failure criteria in meridian plane.
Rys. 4. Różne kryteria zniszczenia w przekroju południkowym

to describe the criterion of the material effort in energetic form [3]. Below we present some representative criteria that depend on various number of parameters.

3.2.1. The Huber-Mises-Hencky (HMH) failure criterion

The criterion assumes that the strain energy of distortion (energy of deviatoric state) is only responsible for failure of material [26]. It is expressed in the following form:

$$f(J_2) = J_2 - k^2 = 0. \tag{3.13}$$

It assumes only one constitutive parameter k, which can be computed form the compressive strength of concrete f_c:

$$k = \frac{f_c}{\sqrt{3}}. \tag{3.14}$$

Taking into account the equations 2-3, the strain energy of distortion, which decides on the material failure, is as following:

$$W_2 = \frac{(1+v)}{E}\frac{f_c^2}{3} = 0.012 MJ/m^3. \tag{3.15}$$

In the space defined by the strain energy of distortion W_2 and the volume change of strain energy W_1, this criterion for the data: compressive strength $f_c = 30MPa$,

Young modulus $E = 30e3MPa$ and Poisson ratio $v = 0.2$ is presented in Fig. 2 as red line (parallel to W_1 axis). Additionally, the shapes of this condition in plane stress case and in meridian plane are shown in Figs 3 and 4 as red lines.

3.2.2. The Drucker-Prager (DP) failure criterion

The criterion takes into consideration additionally the influence of the first invariants of stress state I_1 and the volume change strain energy density [6, 23]. The criterion is written in the form:

$$f(I_1, J_2) = mI_1 + \sqrt{J_2} - k = 0. \tag{3.16}$$

To identify the two constitutive parameters m and k, the using of the two points $(f_t, 0)$ and $(-f_c, 0)$ is necessary. It is required that the failure surface passes through both points. This condition is satisfied for the pair of numbers (m, k) in the form:

$$\begin{cases} m = \dfrac{(f_c - f_t)}{\sqrt{3}(f_c + f_t)} \\ k = \dfrac{2f_c f_t}{\sqrt{3}(f_c + f_t)} \end{cases}. \tag{3.17}$$

Assuming $f_c = 30MPa$ and $f_t = 3MPa$, we obtain two parameters $m = 0.47$ and $k = 3.15$. The strain energy of distortion which decides on the failure in DP criterion is dependent on the volume change strain energy according to the following expression:

$$W_2 = \begin{cases} \dfrac{1+v}{E}k^2 + 2mk\dfrac{1+v}{E}\sqrt{\dfrac{6E}{1-2v}W_1} + 6m^2\dfrac{1+v}{1-2v}W_1 & I_1 < 0 \\ \dfrac{1+v}{E}k^2 - 2mk\dfrac{1+v}{E}\sqrt{\dfrac{6E}{1-2v}W_1} + 6m^2\dfrac{1+v}{1-2v}W_1 & I_1 \geq 0 \end{cases}. \tag{3.18}$$

In Figs 2-4, the failure criterion in space $W_2 - W_1$, in plane stress conditions and in meridian plane, for $f_c = 30MPa$, $f_t = 3MPa$, $E = 30e3MPa$, and $v = 0.2$ are shown by orange line.

3.2.3. The Bresler-Pister (BP) failure criterion

The BP criterion describes the strength in advance state of stress and takes into account both the strain energy of distortion and the volume change strain energy density [2]. It is presented in the following form:

$$f(I_1, J_2) = A + BI_1 + C(I_1)^2 - \sqrt{J_2} = 0. \tag{3.19}$$

This criterion is depends on 3 independent parameters. For identification of these constitutive parameters A, B and C, it is necessary to use three points defined by experimental tests, there are $(f_t, 0)$, $(-f_c, 0)$ and $(-f_bc, -f_bc)$, where f_bc is the strength of concrete for biaxial uniform compression. The criterion passes thought three identification points and defines the three parameters (A, B, C) in the form:

$$\left\{\begin{array}{l} A = \dfrac{(f_c f_t f_{bc})\,(f_t + 3f_c + 8f_{bc})}{\sqrt{3}\,(f_c + f_t)\,(2f_{bc} - f_c)\,(2f_{bc} + f_t)} \\ B = \dfrac{(f_c - f_t)\left(f_{bc}f_c + f_{bc}f_t - f_t f_c - 4f_{bc}^2\right)}{\sqrt{3}\,(f_c + f_t)\,(2f_{bc} - f_c)\,(2f_{bc} + f_t)} \\ C = \dfrac{(3f_{bc}f_t - f_{bc}f_c - 2f_t f_c)}{\sqrt{3}\,(f_c + f_t)\,(2f_{bc} - f_c)\,(2f_{bc} + f_t)} \end{array}\right. . \tag{3.20}$$

Assuming $f_c = 30MPa$, $f_t = 3MPa$ and $f_{bc} = 33.6MPa$, the three constitutive parameters are of values $A = 3.6832$, $B = -0.6326$ and $C = -0.0059$. The strain energy of distortion as a function of the volume change strain energy is presented by the equation:

$$W_2 = \left\{\begin{array}{ll} a\left(\begin{array}{c} A^2 - 2AB\sqrt{bW_1} - 2ACbW_1 + \\ 2BC\sqrt{(bW_1)^3} + B^2 bW_1 + C^2 (bW_1)^2 \end{array}\right) & I_1 < 0 \\ a\left(\begin{array}{c} A^2 + 2AB\sqrt{bW_1} + 2ACbW_1 + \\ 2BC\sqrt{(bW_1)^3} + B^2 bW_1 + C^2 (bW_1)^2 \end{array}\right) & I_1 \geq 0 \end{array}\right. , \tag{3.21}$$

where:

$$a = \frac{1+v}{E}, \quad b = \frac{6E}{1-2v}. \tag{3.22}$$

In Figs 2-4 we have presented the curves of the Bresler-Pister failure criterion in space $W_2 - W_1$, in plane stress conditions and in meridian plane by green lines for comparison with earlier failure criteria.

3.2.4. The Mróz (M) failure criterion

The three parameters failure criterion with ellipse shape in meridian plane was introduced by Mróz [15] in the form:

$$f(I_1, J_2) = (I_1 - A)^2 + BJ_2 - C = 0. \tag{3.23}$$

The same identification points like in the cases of the Burzyński and the Bresler-Pister failure criteria were used to identify three constitutive parameters A, B and C. The conditions are satisfied for the following three numbers (A, B, C):

$$\begin{cases} A = \dfrac{3}{2}\dfrac{(f_c - f_t) f_{bc}^2}{\Omega} \\ B = -3\dfrac{3f_{bc}^2 + \Omega}{\Omega} \\ C = \dfrac{\Omega\left[4\Omega f_t - 12 f_t f_{bc}^2 (f_c - 2f_t) - 4\Omega f_t^2\right] + 9(f_c - f_t)^2 f_{bc}^4}{4\Omega^2} \end{cases}, \tag{3.24}$$

where:

$$\Omega = (f_{bc} - f_c)(f_{bc} - f_t) - (f_c - f_t) f_{bc}. \tag{3.25}$$

Assuming as before $f_c = 30MPa$, $f_t = 3MPa$ and $f_{bc} = 33.6MPa$, the three constitutive parameters are $A = -58.96$, $B = 10.10$ and $C = 3863.82$. The strain energy of distortion as a function of the volume change strain energy is presented by the equation:

$$W_2 = \begin{cases} \dfrac{a}{B}\left[C - \left(\sqrt{bW_1} - A\right)^2\right] I_1 \geq 0 \\ \dfrac{a}{B}\left[C - \left(-\sqrt{bW_1} - A\right)^2\right] I_1 < 0 \end{cases} \tag{3.26}$$

where:

$$a = \frac{1+v}{E}, \quad b = \frac{6E}{1-2v}. \tag{3.27}$$

The Mróz failure criterion in space $W_2 - W_1$, in plane stress conditions and in meridian plane is presented in Figs 2-4 by black continuous lines. The M criterion is identical with the Burzyński failure criterion for the same identification points so in the future will be called the Burzyński-Mróz failure criterion.

3.2.5. The Willam-Warnke (WW) failure criterion

The criterion introduced for concrete by Willam-Warnke [28] in three dimensional stress state is proposed in the form:

$$f(I_1, J_2, J_3) = \frac{1}{3z}\frac{I_1}{f_c} + \sqrt{\frac{2}{5}}\frac{1}{r(\theta)}\frac{\sqrt{J_2}}{f_c} - 1, \tag{3.28}$$

where:

$$r(\theta) = \frac{2r_c\left(r_c^2 - r_t^2\right)\cos\theta + r_c\left(2r_t - r_c\right)\sqrt{4\left(r_c^2 - r_t^2\right)\cos^2\theta + 5r_t^2 - 4r_c r_t}}{4\left(r_c^2 - r_t^2\right)\cos^2\theta + \left(r_c - 2r_t\right)^2}, \tag{3.29}$$

for:

$$\begin{aligned} \theta &= \frac{1}{3}\cos^{-1}\left(\frac{3\sqrt{3}}{2}\frac{J_3}{\sqrt[2]{J_2^3}}\right), \\ \cos\theta &= \frac{2\sigma_1 - \sigma_2 - \sigma_3}{\sqrt{2\left[(\sigma_1 - \sigma_2)^2 + (\sigma_2 - \sigma_3)^2 + (\sigma_1 - \sigma_3)^2\right]}}. \end{aligned} \tag{3.30}$$

The identification of the three parameters r_c, r_t and z can be performed based on the same points as before. The values of invariants I_1, J_2 and θ, which correspond to the three identification points $(f_t, 0, 0), (-f_c, 0, 0)$ and $(-f_b c, -f_b c, 0)$, are collected in Tab. 2.

Table 2

Data for identification of Willam-Warnke criterion parameters.
Dane do identyfikacji parametrów kryterium Willama-Warnkego

Point	I_1	J_2	θ	$r(\theta)$
$(\sigma_1, \sigma_2, \sigma_3) = (f_t, 0, 0)$	f_t	$\frac{f_t^2}{3}$	0^0	r_t
$(\sigma_1, \sigma_2, \sigma_3) = (-f_c, 0, 0)$	$-f_c$	$\frac{f_c^2}{3}$	60^0	r_c
$(\sigma_1, \sigma_2, \sigma_3) = (-f_{bc}, -f_{bc}, 0)$	$-2f_{bc}$	$\frac{f_{bc}^2}{3}$	0^0	r_t

The three parameters are found in the form:

$$\begin{cases} \mathrm{r_t} = \sqrt{\frac{6}{5}}\left[\frac{f_{bc}f_t}{f_c\left(2f_{bc} + f_t\right)}\right] \\ r_c = \sqrt{\frac{6}{5}}\left[\frac{f_{bc}f_t}{3f_{bc}f_t + f_c\left(f_{bc} - f_t\right)}\right] \\ z = \frac{f_{bc}f_t}{f_c\left(f_{bc} - f_t\right)} \end{cases}, \tag{3.31}$$

The failure surface passes thought the three identification points. Assuming $f_c = 30MPa, f_t = 3MPa$ and $f_{bc} = 33.6MPa$, the three parameters have the values $r_t = 0.0524316, r_c = 0.090479$ and $z = 0.1098039$. The strain energy density of distortion as a function of the volume change strain energy density for the Willam-Warnke failure criterion is presented by equation:

$$W_2 = \begin{cases} a\left[\frac{5}{2}f_c^2 r^2(\theta) - \frac{5}{3}\frac{f_c r^2(\theta)}{z}\sqrt{bW_1} + \frac{5}{18}\frac{r^2(\theta)}{z^2}\right] & I_1 \geq 0 \\ a\left[\frac{5}{2}f_c^2 r^2(\theta) + \frac{5}{3}\frac{f_c r^2(\theta)}{z}\sqrt{bW_1} + \frac{5}{18}\frac{r^2(\theta)}{z^2}\right] & I_1 < 0 \end{cases}, \tag{3.32}$$

where:

$$a = \frac{1+v}{E} \quad \text{and} \quad b = \frac{6E}{1-2v}. \tag{3.33}$$

In Figs 2-4 the curves of the Willam-Warnke failure criterion is presented by black dotted lines (in space $W_2 - W_1$, in plane stress conditions and in meridian plane). In that case, in the deviatoric plane is curve assembled from the parts of ellipse and it is necessary to use in Eq. (3.32) proper value of $r(\theta)$, as in Tab. 2. According to Eq. (3.29) $r(\theta)$, is changing from r_t to r_c.

3.2.6. The Podgórski (P) failure criterion

There are exist many others criteria, which have more parameters. The last one failure criterion which we decided to discuss has five parameters and was proposed for advanced state of stress by Podgórski [22] in the form:

$$f(I_1, J_2, J_3) = \frac{1}{3}I_1 - A + BP(J)\sqrt{\frac{2}{3}J_2} + \frac{2}{3}CJ_2 = 0, \tag{3.34}$$

where:

$$P(J) = \cos\left(\frac{1}{3}\cos^{-1} DJ - E\right), \tag{3.35}$$

while:

$$J = \cos(3\theta) = \frac{3\sqrt{3}}{2}\frac{J_3}{J_2^{3/2}}. \tag{3.36}$$

Table 3

Data for identification of Podgórski failure criterion parameters.
Dane do identyfikacji parametrów kryterium Podgórskiego

Points	I_1	J_2	J	$P(J)$
$(\sigma_1,\sigma_2,\sigma_3)=(f_t,0,0)$	f_t	$\frac{f_t^2}{3}$	1	$\cos\left(\frac{1}{3}\cos^{-1}D-E\right)$
$(\sigma_1,\sigma_2,\sigma_3)=(-f_c,0,0)$	$-f_c$	$\frac{f_c^2}{3}$	-1	$\cos\left(\frac{1}{3}\cos^{-1}-D-E\right)$
$(\sigma_1,\sigma_2,\sigma_3)=(-f_{bc},-f_{bc},0)$	$-2f_{bc}$	$\frac{f_{bc}^2}{3}$	1	$\cos\left(\frac{1}{3}\cos^{-1}D-E\right)$
$(\sigma_1,\sigma_2,\sigma_3)=(-f_{cc},-1/2f_{cc},0)$	$-\frac{3}{2}f_{cc}$	$\frac{1}{4}f_{cc}^2$	0	$\cos\left(\frac{1}{3}\cos^{-1}0-E\right)$
$(\sigma_1,\sigma_2,\sigma_3)=(f_{tt},f_{tt},f_{tt})$	$3f_{tt}$	0	–	–

The identification of five parameters A, B, C, D and E is performed based on five identification points $(f_t,0,0),(-f_c,0,0),(-f_{bc},-f_{bc},0),(-f_{cc},-1/2f_{cc},0)$ and (f_{tt},f_{tt},f_{tt}). The values of invariants for those points are collected in Tab. 3.

The system of equations, which should be solved to compute material parameters, is as follows:

$$
\begin{cases}
\frac{1}{3}f_t - A + B\cos\left(\frac{1}{3}\cos^{-1}D-E\right)\frac{\sqrt{2}}{3}f_t + \frac{2}{3}C\frac{f_t^2}{3} = 0 \\
-\frac{1}{3}f_c - A + B\cos bc\left(\frac{1}{3}\cos^{-1}-D-E\right)\frac{\sqrt{2}}{3}f_c + \frac{2}{3}C\frac{f_c^2}{3} = 0 \\
-\frac{2}{3}f_{bc} - A + B\cos\left(\frac{1}{3}\cos^{-1}D-E\right)\frac{\sqrt{2}}{3}f_{bc} + \frac{2}{3}C\frac{f_{bc}^2}{3} = 0 \\
-\frac{1}{2}f_{cc} - A + B\cos\left(\frac{1}{3}\cos^{-1}0-E\right)\frac{1}{\sqrt{6}}f_{cc} + \frac{2}{3}C\frac{f_{cc}^2}{4} = 0 \\
f_{tt} - A = 0
\end{cases}
\tag{3.37}
$$

The above system of Eq. (3.37) is solved iteratively by Newton method. Assuming data: $f_c = 30MPa, f_t = 3MPa, f_{bc} = 33.6MPa, f_{cc} = 36MPa$ and $f_{tt} = 3MPa$, the five constitutive parameters $A = 3, B = 1.4276, C = 0.0112, D = 1$ and $E = 0.03902$ are specified. The criterion has four identification points in plane stress conditions that are why the shape in this plane (Fig. 3) is in good correlation with experimental data [16].

The strain energy of distortion which decides on the failure criterion is the following function of the volume change strain energy:

$$W_2 = \left(\frac{-BP(J)\sqrt{\frac{2}{3}a} + \sqrt{\Delta}}{\frac{4}{3}Ca} \right)^2, \tag{3.38}$$

where:

$$a = \frac{E}{1+v} \quad \text{and} \quad b = \frac{6E}{1-2v}. \tag{3.39}$$

While Δ is:

$$\Delta = \begin{cases} \frac{2}{3}aB^2P^2(J) - 4\left(\frac{2}{3}Ca\right)\left(\frac{1}{3}\sqrt{bW_1} - A\right) & I_1 \geq 0 \\ \frac{2}{3}aB^2P^2(J) - 4\left(\frac{2}{3}Ca\right)\left(-\frac{1}{3}\sqrt{bW_1} - A\right) & I_1 < 0 \end{cases}. \tag{3.40}$$

4. Modelling of damage and failure

The proper description of concrete failure is important, particularly if we think of concrete behaviour in advanced states of deformations. In the concrete, because of the evolution of existing micro-cracks, the softening appears. This effect, on the ground of continuum mechanics is called damage. Specifically this problem appears in concrete during tension, while proceed the localization of deformation phenomena. From the mathematical point of view, for quasi-static behavior the type of the system of partial differential equations, which govern the process, is changed (from elliptical to hyperbolic) and the problem looses the well-posedness. In consequence, the solution is dependent on the discretization in pathological way [21]. This problem can be regularized in different methods.

4.1. Concrete damage plasticity model

The numerical analysis of initial boundary-value problem with localization of deformations needs a complex constitutive material modeling. In Concrete Damage Plasticity model, two scalar variables are used to describe the damage of concrete, in tension and in compression. Scalar damage was introduced firstly to creep modeling [14] The fundamental problem in numerical analysis of concrete and reinforced concrete structures is the description of the proper mechanism of failure and its load capacity. The constitutive equation of concrete with scalar damage [14,17] is as follows:

$$\sigma = (1-d)\, D_0^{el} : \left(\varepsilon - \varepsilon^{pl}\right) = D^{el} : \left(\varepsilon - \varepsilon^{pl}\right), \tag{4.1}$$

where σ is Cauchy stress tensor, d is a scalar variable of damage (connected with the stiffness degradation), ε is a strain tensor, D_0^{el} is the tensor of the initial material stiffness and $D^e l = (1-d)D_0^e l$ is degraded tensor of material stiffness. It is necessary to define the effective stress measure based on Eq. (4.1):

$$\bar{\sigma} = D_0^{el} : \left(\varepsilon - \varepsilon^{pl}\right), \tag{4.2}$$

where ε^{pl} is tensor of plastic strain. The evolution of damage variable is defined by:

$$d = d(\bar{\sigma}, \bar{\varepsilon}^p l). \tag{4.3}$$

The scalar variable d is a function of effective stress $\bar{\sigma}$ and equivalent plastic strain $\bar{\varepsilon}^{pl}$. The tensor of initial material stiffness is isotropic and during deformation is still isotropic but the elements of this tensor are multiplied by scalar $(1-d)$. The damage of material in tension d_t and in compression d_c is defined independent through two variables $\bar{\varepsilon}_C^p l$ and $\bar{\varepsilon}_T^p l$, which describe the equivalent strain in compression and in tension. Their evolution is specified by:

$$\begin{gathered} \bar{\varepsilon}^{pl} = \begin{bmatrix} \bar{\varepsilon}_S^{pl} \\ \bar{\varepsilon}_R^{pl} \end{bmatrix}, \\ \dot{\bar{\varepsilon}}^{pl} = h\left(\bar{\sigma}, \bar{\varepsilon}^{pl}\right) \dot{\varepsilon}^{pl}. \end{gathered} \tag{4.4}$$

The cracking (in tension) and crushing (in compression) are defined by increasing of the hardening, softening, variables. These variables control the evolution of the loading function and degradation of the material stiffness. The loading function as a function of stress and effective plastic strain describes also the level of damage. For inviscid plasticity with damage material model, the state of stress and strain must satisfy the condition:

$$F\left(\sigma, \bar{\varepsilon}^{pl}\right) \leq 0. \tag{4.5}$$

The plastic flow is defined by plastic flow potential function $G(\sigma)$ and nonassociated flow rule in the form:

$$\dot{\varepsilon}^{pl} = \dot{\lambda} \frac{\partial G(\sigma)}{\partial \sigma}. \tag{4.6}$$

The concrete damage plasticity model is the one of several possibilities. The proper estimation of constitutive parameters from experimental results can guarantee qualitative and quantitative quality of the constitutive model.

4.1.1. Loading function

The loading function [17] used in the model has the form:

$$F(\sigma) = \frac{1}{1-a}\left[\sqrt{3J_2} + \alpha I_1 + \beta\langle\sigma_{\max}\rangle - \gamma\langle-\sigma_{\max}\rangle\right] - f_c, \tag{4.7}$$

The parameters α, β and γ decide on the shape of the function in stress space. The identification of these parameters is crucial. In the case of uniform biaxial compression $(-f_{bc}, -f_{bc}, 0)$ the terms with β and γ disappear in Eq. (4.7), because both $\langle\sigma_{\max}\rangle$ and $\langle-\sigma_{\max}\rangle$ are equal zero (while $\sigma_{\max} = 0$ and the Macauley bracket definition is $\langle * \rangle = \frac{1}{2}(|*| + *)$). In this case the first invariant of stress tensor I_1 is equal $-2f_{bc}$ but the second invariant of stress deviator J_2 is equal $(f_{bc}^2)/3$. Then the Eq. (4.7) takes the shape:

$$\frac{1}{1-\alpha}\left[\sqrt{3\frac{f_{bc}^2}{3}} - 2\alpha f_{bc}\right] = f_c, \tag{4.8}$$

and after conversion we arrived at the dependence:

$$\alpha = \frac{(f_{bc}/f_c) - 1}{2(f_{bc}/f_c) - 1}. \tag{4.9}$$

This dependence serves to determine the parameter α, based on ratio of two strengths (biaxial compression f_{bc} and uniaxial compression f_c). The parameter β is identified based on point $(f_t, 0, 0)$. In this case $\langle\sigma_{\max}\rangle = \langle f_t\rangle = f_t$ and the Eq. (4.7) has the form:

$$\frac{1}{1-\alpha}\left[\sqrt{3\frac{f_t^2}{3}} + \alpha f_t + \beta f_t\right] = f_c, \tag{4.10}$$

because the first invariant of stress tensor I_1 is equal f_t and the second J_2 is equal $(f_t^2)/3$. In this case it is possible to compute β according to the dependence:

$$\beta = \frac{f_c}{f_t}(1-\alpha) - (1-\alpha). \tag{4.11}$$

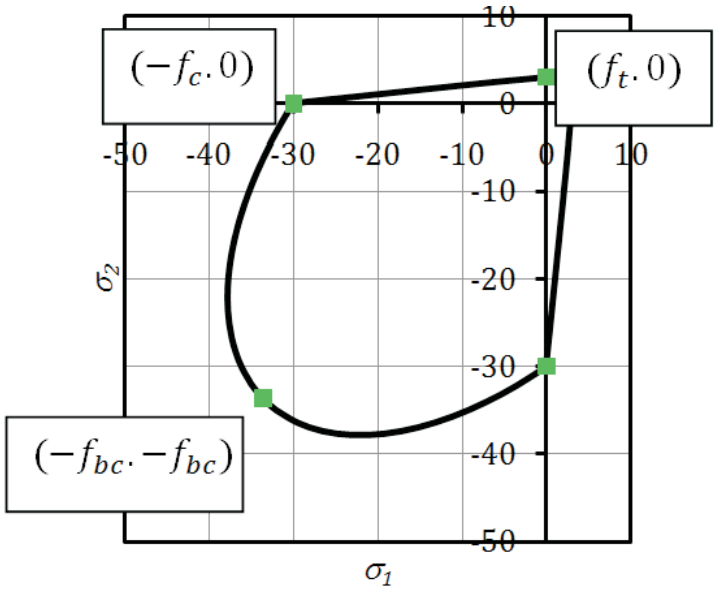

Fig. 5. Lubliner loading function in plane stress conditions.
Rys. 5. Funkcja obciążenia Lublinera w płaskim stanie naprężenia

In plane stress conditions only two parameters decide on the shape of the loading function, that are α and β. The shape is presented in Fig. 5. If we substitute to equation (4.7) invariants I_1 and J_2 correspond to point $(-f_c, 0, 0)$, this equation is satisfied identity. The Lubliner loading function is presented in Fig. 5 in plane stress conditions. The parameter γ appears only in three-axial state of stress if $\sigma_{\max} < 0$. Its influence is visible in meridian plane. In view of the specific and different nature of the loading function (4.7) in relation to the earlier presented criteria, in Fig. 6 the shape of the criterion in meridian plane $r - \xi$ is shown. The important are the results of experiments (Launay & Gachon, 1971), which one marked by ◗ in Fig. 6. The two meridians: tensile meridian TM ($r < 0$) and compressive meridian CM ($r > 0$) are presented in Fig. 6. Important is the ratio of both radiuses r for a specific ξ:

$$\rho = \frac{r_{TM}}{r_{CM}} \quad \text{for} \quad \xi \tag{4.12}$$

The definition of maximum principal stresses (Abbo & Sloan [1]) for both meridians is necessary to construct the general equation of both meridians:

$$\sigma_{\max} = \begin{cases} \frac{1}{3}\left(I_1 + 2\sqrt{3J_2}\right) & \text{for} \quad r_{TM} \\ \frac{1}{3}\left(I_1 + 2\sqrt{3J_2}\right) & \text{for} \quad r_{CM} \end{cases} \tag{4.13}$$

Then the equation of both meridians is the following:

$$r_{TM} = \begin{cases} \dfrac{\sqrt{6}}{3}\dfrac{(1-\alpha)\,f_c - (\alpha+\gamma/3)\,\sqrt{3}\xi}{1+2\gamma/3} \\ \dfrac{\sqrt{6}}{3}\dfrac{(1-\alpha)\,f_c - (\alpha+\beta/3)\,\sqrt{3}\xi}{1+2\beta/3} \end{cases} \quad \text{for} \quad \begin{array}{c} r < -\dfrac{\xi}{\sqrt{2}} \\ \square \\ r \geq -\dfrac{\xi}{\sqrt{2}} \end{array}, \tag{4.14}$$

$$r_{CM} = \begin{cases} \dfrac{\sqrt{6}}{3}\dfrac{(1-\alpha)\,f_c - (\alpha+\gamma/3)\,\sqrt{3}\xi}{1+\gamma/3} \\ \dfrac{\sqrt{6}}{3}\dfrac{(1-\alpha)\,f_c - (\alpha+\beta/3)\,\sqrt{3}\xi}{1+\beta/3} \end{cases} \quad \text{for} \quad \begin{array}{c} r < -\dfrac{2\xi}{\sqrt{2}} \\ \square \\ r \geq -\dfrac{2\xi}{\sqrt{2}} \end{array}, \tag{4.15}$$

From the analysis of the Eq. (4.7) it appears, that thanks to use the Macauley bracket, it is required to define the meridian equations independently in two zones: compressive $\sigma_{\max} < 0$ and tensile $\sigma_{\max} > 0$. The corresponding straight lines are printed in Fig. 6 by dashed lines. In addition, on the chart the identification points are marked by ■. All three points lie on the meridians in the zone, where influence has only parameters α and β, what validates the identification procedure. In the zone of three-axial compression, where $\langle -\sigma_{\max} \rangle \neq 0$, in the Eq. (4.12) is necessary to take into account the proper value of r Eqs (4.14)-(4.15), what leads to the dependence:

$$\rho = \frac{\gamma + 3}{2\gamma + 3}. \tag{4.16}$$

After transformation of the above formula, we can obtain:

$$\gamma = \frac{3\,(1-\rho)}{2\rho - 1}. \tag{4.17}$$

Therefore the parameter γ is identified by the global fit into the experimental data in three-axial compression zone. In Fig. 6 the experimental results are presented [4]. These results give a parameter which varies between 0.64 and 0.8 depending on research laboratory.

In accordance with the above-mentioned considerations, the evolution of $F(\sigma)$ depending on $\bar{\varepsilon}^{pl}$ can be taken into account in Eq. (4.7). We decided to complete this in the following way:

To make changeable the parameter β form the actual values of effective compressive stress $\bar{\sigma}_C$ and effective tensile stress $\bar{\sigma}_T$, which are the functions of $\bar{\varepsilon}_C^{pl}$ and $\bar{\varepsilon}_T^{pl}$:

$$\beta = \frac{\bar{\sigma}_S\left(\bar{\varepsilon}_S^{pl}\right)}{\bar{\sigma}_R\left(\bar{\varepsilon}_R^{pl}\right)}(1-\alpha) - (1-\alpha), \tag{4.18}$$

To replace the parameter f_c by the function $\bar{\sigma}_C\left(\bar{\varepsilon}_C^{pl}\right)$:

$$f_c = \bar{\sigma}_S\left(\bar{\varepsilon}_S^{pl}\right). \tag{4.19}$$

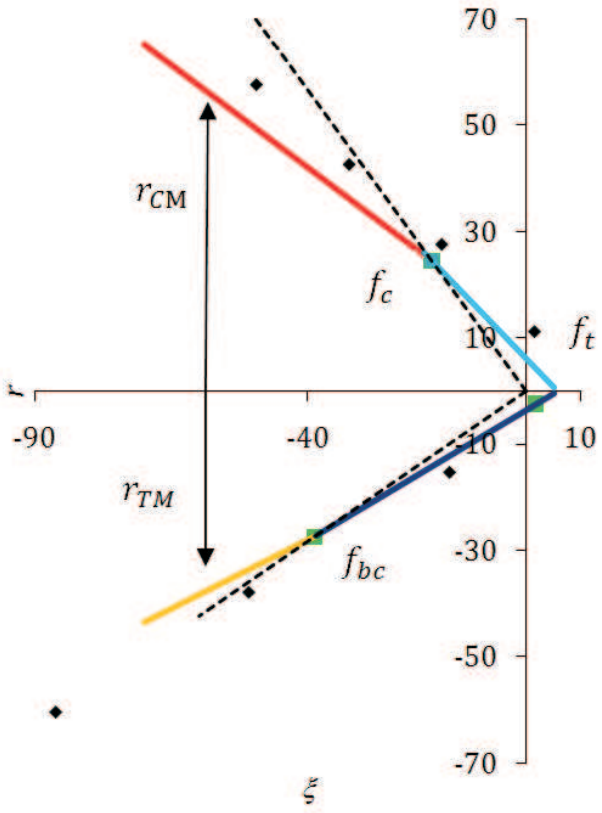

Fig. 6. Meridian plane of Lubliner loading function.
Rys. 6. Funkcja obciążenia Lublinera w przekroju południkowym

4.1.2. Plastic potential surface

The concrete damage plasticity model assumes the use of nonassociated flow rule. Therefore this section discusses the method of identification of two parameters ψ, ϵ of plastic potential function G. The Drucker-Prager hyperbolic function [1] in the form:

$$G(\sigma) = \sqrt{(f_c - \epsilon f_t \tan\psi)^2 + q^2} + p\tan\psi - f_c = 0, \tag{4.20}$$

where $p = \frac{1}{3}I_1$ is the effective hydrostatic pressure and $q^2 = 3J_2$ is HMH effective stress. The two parameters ψ, ϵ occur in the above equation. Their influence on the shape of the plastic potential function is shown in Fig. 7.

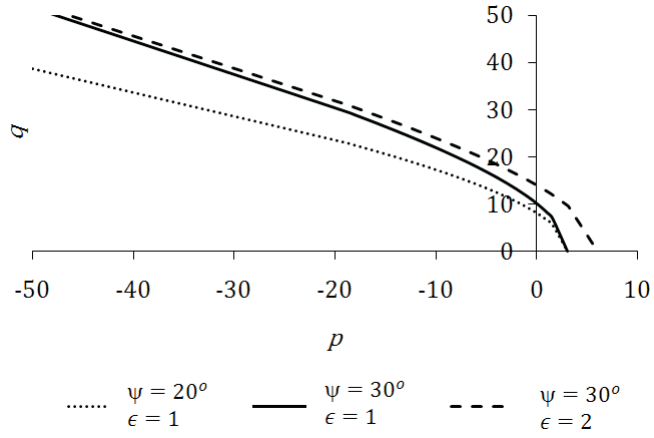

Fig. 7. Plastic potential function.
Rys. 7. Funkcja potencjału plastycznego

The two parameters ψ, ϵ are identified through global matching in plane p-q by using the last square method [13].

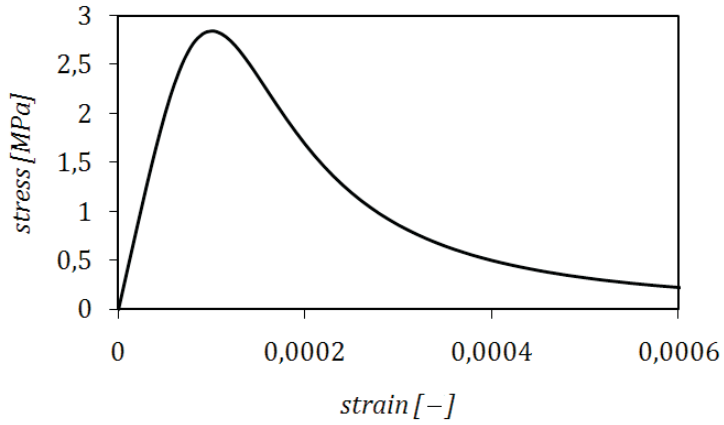

Fig. 8. Uniaxial compression of concrete [26].
Rys. 8. Jednoosiowe ściskanie betonu [26]

4.2. IDENTIFICATION OF THE CONSTITUTIVE PARAMETERS

The general idea of the concrete damage plasticity model was presented. The meaning and interpretation of the parameter were also explained. The identification of parameters for concrete class B50 based on laboratory tests is now discussed in details. The most important test which proves the class of concrete is uniaxial compression test. The corresponding curve is presented in Fig. 8. The important is also test for uniaxial tension, which gives the results presented in Fig. 9. In addition, to match the parameters ψ, ϵ of the plastic flow potential function, the well known experimental results (Swanson & Green [25]) are used (Fig. 10). These are the results of three-axial compression (see Fig. 10), which are superposition of hydrostatic compression with p = 0.0, 6.9, 13.8 MPa and additional compression in 3-3 direction up to failure. The Kupfer curve (Fig. 1) is also necessary to describe the parameters of the loading function.

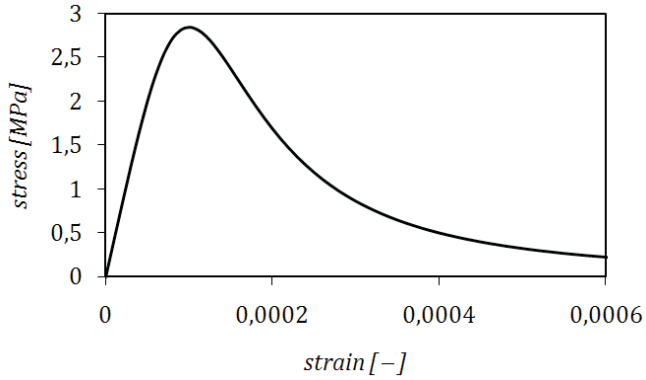

Fig. 9. Uniaxial tension of concrete [26].
Rys. 9. Jednoosiowe rozciąganie betonu [26]

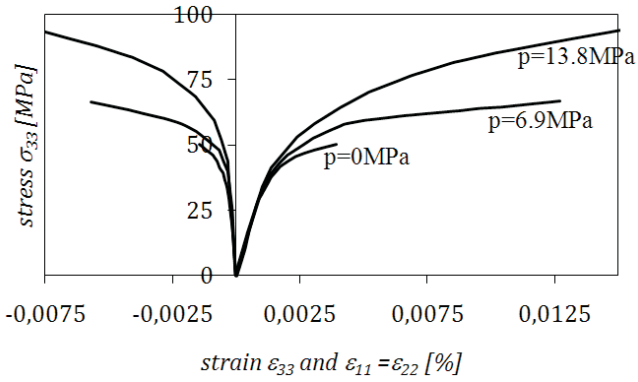

Fig. 10. Triaxial compression of concrete [25].
Rys. 10. Trójosiowe ściskanie betonu [25]

One can assume that the concrete behaves linearly elastic in compression up to $0.6f_c$ and in tension to value f_t. In the elastic zone, the Young modulus is $E_0 = 18.5GPa$ and the Poisson ratio is $\nu = 0.19$. It is the result of quotients of the both coordinates in point ● in Fig. 11 that is stress 30 MPa and strain 0.001622. This point is the elastic limit and from that point to the stress 50 MPa, the concrete still hardens. In this range possible unloading is along the line which is parallel to the red segment with the slope equals to E_0. To define the curve of hardening (softening) in compression, it is necessary to use maximal number of point with coordinates are $\left(\bar{\varepsilon}_C^{nl}, \bar{\sigma}_C\right)$, where $\bar{\varepsilon}_C^{nl}$ is inelastic compressive strain, which is computed through the subtracting from the total strain $\bar{\varepsilon}_C^{nl}$ the elastic part $\bar{\varepsilon}_C^{el}$. When the stress reaches 50 MPa the concrete in compression starts to soften, what is connected with degradation of its stiffness. The degradation of concrete stiffness is experimentally observed, what is particularly visible during cyclic loading (Fig. 8) when the change of stiffness appears after unloading. The decreasing of the model stiffness is connected with increasing of the damage variable in compression. The method of describing the points $\left(\bar{\varepsilon}_C^{nl}, \bar{\sigma}_C\right)$ bases on experimental curve is presented for one example point marked in Fig. 11 by dot ● with numbers 1, 2, 3 and 4. The coordinates ● $1(\bar{\varepsilon}_C = 0.0055, \bar{\sigma}_C = 30)$ are read directly from the chart in Fig. 11. The abscissa 0.0055 corresponds to point ● 2. It is the total strain $\bar{\varepsilon}_C$. Based on ● 1 we compute inelastic strain $\bar{\varepsilon}_C^{nl}$, which is the abscissa of the point ● 3. We assume that unloading runs parallel to initial value of E_0. In this case we use formula $\bar{\varepsilon}_C^{nl} = \bar{\varepsilon}_C - \bar{\sigma}_C/E_0$. For this case the abscissa $\bar{\varepsilon}_C^{nl}$ of the point ● 3 is equal 0.0039. Therefore, the identified point of material card has coordinates $(\bar{\varepsilon}_C^n l = 0.0039, \bar{\sigma}_C = 30)$. The points which define the evolution of damage variable in space $\bar{\varepsilon}_C^{nl}, d_C$ and degradation of stiffness are described in the following: the abscissa $\bar{\varepsilon}_C^{nl}$ is identical like earlier but damage variable d_C is equal $(f_c - \bar{\sigma}_C)/f_c$. Based on the information on the values $\bar{\sigma}_C, d_C$ and $\bar{\varepsilon}_C^{nl}$, the plastic strain $\bar{\varepsilon}_C^{pl}$ (point ● 4) is computed according to the following formula:

$$\bar{\varepsilon}_C^{pl} = \bar{\varepsilon}_C^{nl} - \frac{d_C}{1 - d_C} \frac{\bar{\sigma}_C}{E_0}. \tag{4.21}$$

The analogical consideration is also true in the case of tension. In the softening zone there is an inelastic strain localization $\bar{\varepsilon}_T^{nl}$ and in consequence of the plastic strain localization $\bar{\varepsilon}_T^{nl}$, which is connected with degradation of stiffness. The stiffness of concrete corresponding to degradation $\bar{\varepsilon}_T^{pl}$ is equal $(1 - d_T)E_0$. In the softening zone additional constitutive parameter is G_T, which according to the fracture mechanics, describes the energy necessary to open unity crack [11] and the brittle behavior is described not by the curve $\bar{\sigma}_T - \bar{\varepsilon}_T^{pl}$ but by the curve $\bar{\sigma}_T - \bar{u}_T^{pl}$. If the crack width is equal the critical value $\bar{u}_(T - MAX)^{pl}$, the capacity of concrete decrease to zero.

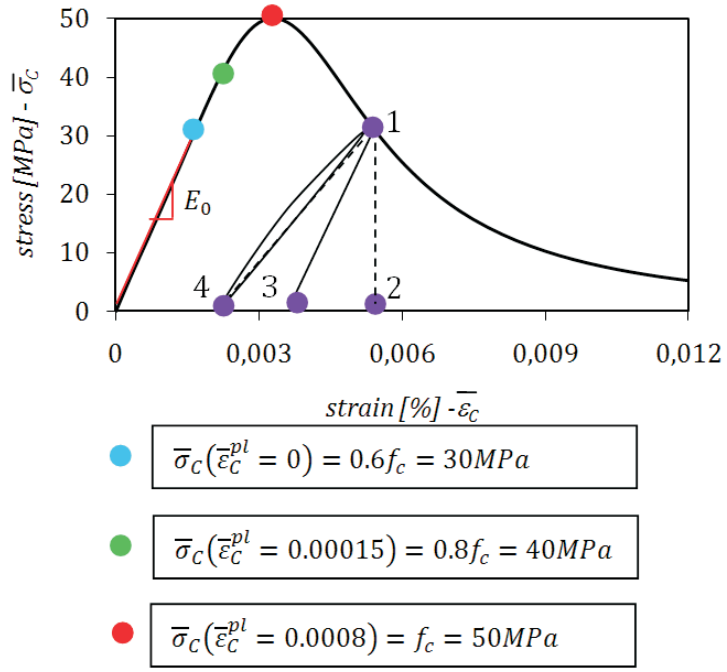

Fig. 11. Stress-strain dependence for compression of concrete damage plasticity model.
Rys. 11. Zależność naprężenie-odkształcenie dla ściskania w modelu betonu plastycznego ze zniszczeniem

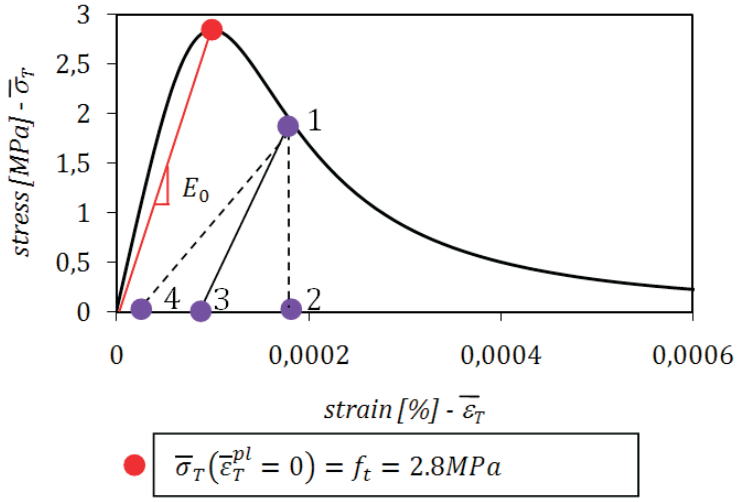

Fig. 12. The stress-strain dependence for tension of concrete damage plasticity model.
Rys. 12. Zależność naprężenie-odkształcenie dla rozciągania w modelu betonu plastycznego ze zniszczeniem

After the cracking, the concrete carries residual stress according to energy of cracking, which is the area under the curve $\bar{\sigma}_T - \bar{u}_T^{pl}$. The absorbed energy by creating of the unity crack is equal:

$$G_T = \int_0^{\bar{u}_{T-MAX}^{pl}} \bar{\sigma}_T d\bar{u}_T^{pl}. \tag{4.22}$$

The function which describes the residual stress after initiation of cracking can be defined in different ways (for example exponential function) but simple linear gives also good results. The following data should be used to describe the linear elastic material up to f_t and then linear softening connected with stiffness degradation up to $\bar{u}_{T-MAX}^{pl}$ (the Critical Cracking Displacement CCD):

Table 4

Tension softening.
Osłabienie w rozciąganiu

$\bar{\sigma}_T$	$\bar{u}_T^{pl}$
2.8 MPa	0
0	$\bar{u}_{T-MAX}^{pl}$

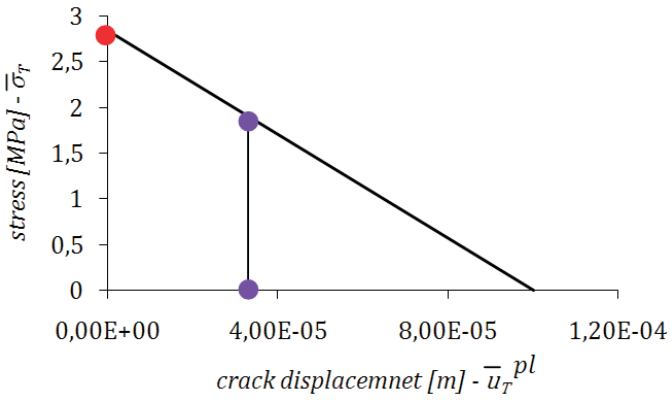

Fig. 13. Linear softening in tension.
Rys. 13. Liniowe osłabienie w rozciąganiu

The maximal degradation of concrete is 0.99. The known are initial equivalent plastic strain in tension in the moment t that is $\bar{\varepsilon}_{(T-t)}^{pl}$ and $d_{(T-t)}$. The next increment of

the equivalent plastic strain in tension $\dot{\bar{\varepsilon}}^{pl}_{T}$ based on unassociated flow role is computed. The next stage is the computation of new equivalent plastic strain in tension:

$$\bar{\varepsilon}^{pl}_{T-t+\Delta t} = \bar{\varepsilon}^{pl}_{T-t} + \dot{\bar{\varepsilon}}^{pl}_{T}. \tag{4.23}$$

If the value $\bar{\varepsilon}^{pl}_{T-t+\Delta t} l_0$ is greater than the critical value $\bar{u}^{pl}_{T-MAX} = \bar{\varepsilon}^{pl}_{(T-CRIT)} l_0$, the computation of damage variable is performed using the following equation:

$$d_{T-t+\Delta t} = d_{T-t} + \dot{\bar{u}}^{pl}_{T} / \bar{u}^{pl}_{T-MAX}. \tag{4.24}$$

In addition, the evolution of loading function according to the evolution of equivalent stress as a function of plastic strain is presented in Fig. 14. The regularization ensures constant dissipation of energy during the cracking, because the strain energy density is independent of the finite element size. The parameters that describe the behaviour of concrete class B50 in compression and in tension are shown in Tab. 5 and 6.

Table 5

Relationship $\bar{\sigma}_C - \bar{\varepsilon}^{nl}_{C}$ and $d_C - \bar{\varepsilon}^{nl}_{C}$.
Zależność $\bar{\sigma}_C - \bar{\varepsilon}^{nl}_{C}$ i $d_C - \bar{\varepsilon}^{nl}_{C}$

$\bar{\sigma}_C$ [MPa]	$\bar{\varepsilon}^{nl}_{C}$	d_C	$\bar{\varepsilon}^{nl}_{C}$
30.0	*0.000099*	*0.0*	*0.000099*
40.0	*0.000154*	*0.0*	*0.000154*
50.0	*0.000762*	*0.0*	*0.000762*
40.0	*0.002558*	*0.2*	*0.002558*
20.0	*0.005675*	*0.6*	*0.005675*
5.0	*0.011733*	*0.9*	*0.011733*

Table 6

Relationship $\bar{\sigma}_T - \bar{\varepsilon}^{nl}_{T}$ and $d_T - \bar{\varepsilon}^{nl}_{T}$.
Zależność $\bar{\sigma}_T - \bar{\varepsilon}^{nl}_{T}$ i $d_T - \bar{\varepsilon}^{nl}_{T}$

$\bar{\sigma}_C$ [MPa]	$\bar{\varepsilon}^{nl}_{C}$	d_C	$\bar{\varepsilon}^{nl}_{C}$
2.800	*0.0*	*0.0*	*0.0*
0.028	*0.0004*	*0.99*	*0.0004*

Additional parameters are α and γ. They describe the shape of the loading surface in the meridian plane and in plane stress conditions according to Figs 5-6 and presented before equations. Based on the Kupfer curve which describes the ratio f_{bc}/f_c as 1.12, a parameter α is equal 0.0967742. The comparison of experimental data in meridian

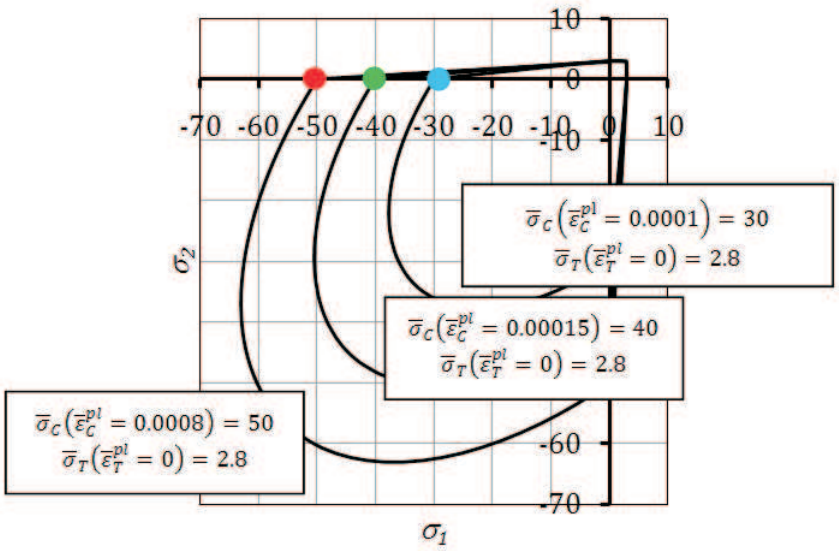

Fig. 14. Evolution of loading function in plane stress conditions.
Rys. 14. Ewolucja funkcji obciążenia w płaskim stanie naprężenia

plane [5] with the shape of the loading function in Fig.6 gives the value of ρ equal 0.666. In this case the parameter which decides the shape of the loading function in meridian plane γ is equal 3. The last stage is the identification of two parameters ψ, ϵ, which describes the shape of plastic flow potential function in meridian plane. The method of identification is the method of global matching. As a basis the well known results of triaxial compression are used [25]. Based on the principal stresses we describe the values of equivalent stresses p and q. In this plane the identification of the parameters is performed based on the last square method, which minimalizes the error in the following form:

$$f = \sum_{t=1}^{4} \left(q_i - q\left(p_i, \psi, \epsilon, f_c, f_t\right)\right)^2 \rightarrow \min . \tag{4.25}$$

The minimization leads to estimation of the parameters ψ, ϵ, which have the values 49° and 1.0, respectively. The shape of plastic potential function together with 4 identification points is shown in Fig. 15.

5. Computational example (four point bending of a concrete notched beam)

The asymmetric four points bending of a single notched concrete beam is an important standard test to test and improve the concrete constitutive models. The failure of the beam is caused by single nonsymmetrical crack, which is presented in Fig. 17. The

Table 7

Identification points of plastic flow potential function.
Punkty identyfikujące funkcji potencjału plastycznego

No	p_i [MPa]	q_i [MPa]	σ_1 [MPa]	σ_2 [MPa]	σ_3 [MPa]
1	2.8	0	2.8	2.8	2.8
2	–16.6	50	0.0	0.0	–50
3	–28.9	66	–6.9	–6.9	–72.9
4	–44.1	91	–13.8	–13.8	–104.8

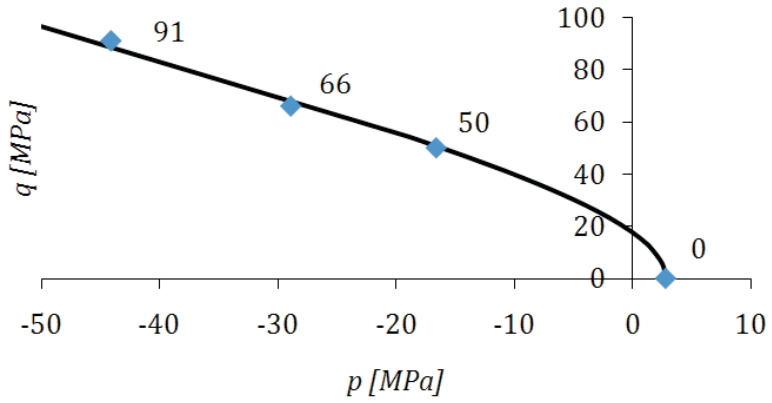

Fig. 15. Plastic flow potential function with identification points.
Rys. 15. Funkcja potencjału plastycznego wraz z punktami identyfikującymi

geometry of the considered concrete beam with boundary conditions is visible in Fig. 16. All dimensions of the beam are specified in millimetres, and the width of the beam is 100 mm. An important element of the test is proper application of single parameter loading as specified in Fig. 16. In numerical simulation [9, 10] the loading was enforced kinematically, like in experiment [24], in order to register the process of damage evolution of the concrete sample. If the loading is transmitted through a monotonically growing force and the critical force is reached, quasi-static process became dynamic and the concrete sample collapses suddenly. As a result, this leads to a sudden loss of static equilibrium and to absence of convergence of the classical Newton-Rapson procedure.

In numerical model, similarly to real experiment, the displacement driven process was enforced. The distance between the force and the central point of applying force to the beam is ten times less than the distance between the force and left point of the force applying. This causes that the loading is carried out exactly the same as in laboratory experiment. The numerical calculations were performed for different sizes of the finite element mesh (CPS4R – four nodes, linear interpolation and plane stress with reduced integration finite element) and different constitutive parameters, particularly governed

the softening process in tension (critical displacement). The characteristic lengths of finite elements are 1, 2 and 5 mm in numerical calculations. For selected discretisation, the influence of the basic numerical parameter, besides tensile strength equals 3.0 MPa that is the critical cracking displacement (CCD)$\bar{u}^{pl}_{(T-MAX)}$ is discussed.

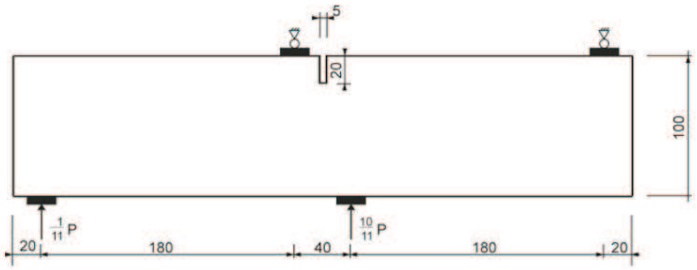

Fig. 16. Geometry and boundary conditions.
Rys. 16. Geometria i warunki brzegowe

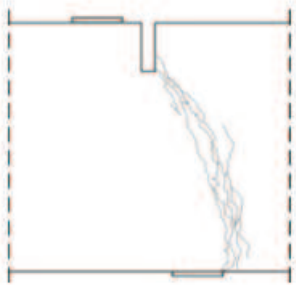

Fig. 17. Failure pattern.
Rys. 17. Mechanizm zniszczenia

In Fig. 18 the relations force and crack mouth sliding displacement for different values of CCD and for fixed element size 0.002 m are presented. It is visible that CCD has the important influence on post-critical behaviour, after reaching the capacity force. The smaller value of CCD corresponds to less cracking energy needed to open the unit crack and more brittle global behaviour of the structure. The relative difference in maximum achieved force is approximately 15% [(45 kN−39 kN)/39 kN·100%]. The next computations were performed for different characteristic finite element lengths. Fig. 19 presents two curves (red and blue) for two element sizes that are 0.001 m and 0.002 m. The difference between the capacity forces for both cases is about 8% [(39 kN−36 kN)/36 kN·100%]. An important conclusion is that presented solution is acceptable, because it does not depend on FEM discretization in pathological way. In addition, in Fig. 19 between the dashed lines the experimental results [24] are

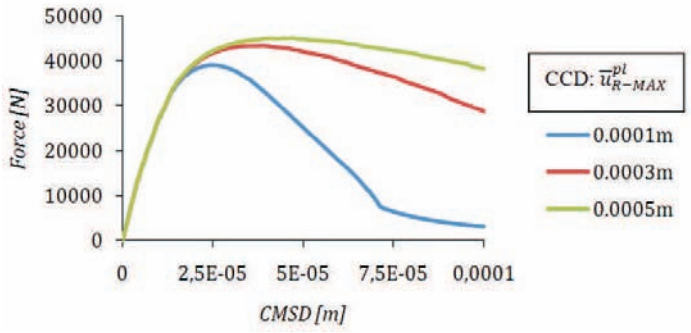

Fig. 18. Influence force- crack mouth sliding displacement for different value of CCD and the element size 0.002m.

Rys. 18. Zależność siła – wzajemne pionowe przemieszczenie punktów w nacięciu dla różnych wartości CCD i wielkości elementu skończonego 0.002m

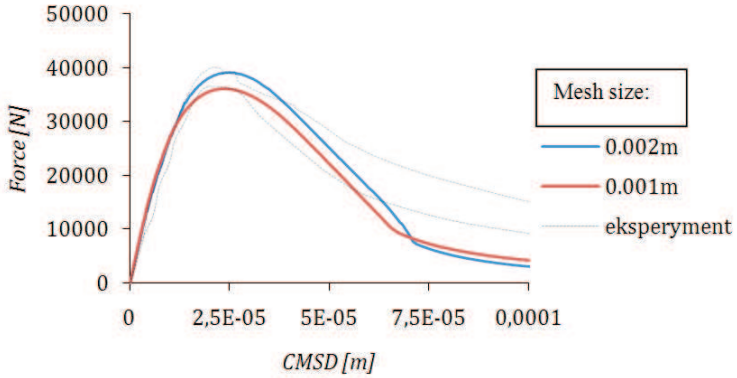

Fig. 19. Comparison with experiment.

Rys. 19. Porównanie z eksperymentem

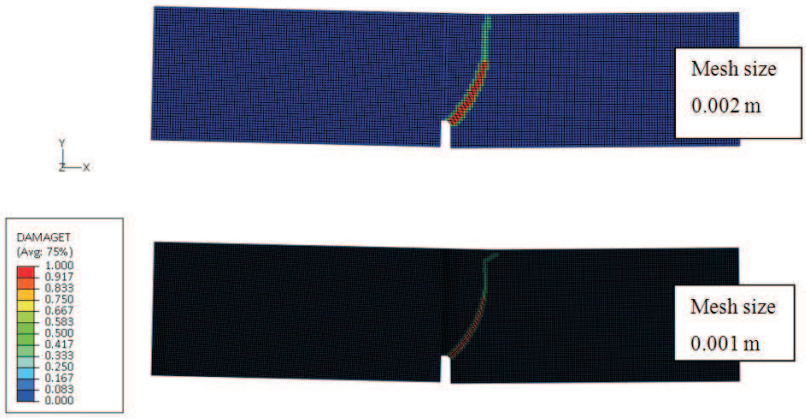

Fig. 20. Comparison of result for both discretisations (distribution of damaget variable).

Rys. 20. Porównanie wyników dla obu dyskretyzacji (rozkład zmiennej damaget)

indicated. The distribution of damage parameter on the final stage of the failure process for both characteristic element sizes is presented in Fig. 20. The displacements are five times scaled and the failure patterns are in agreement with experiments (Fig. 17). Note that in this case, the introduction of internal length scale (regularization) is by defining a constant energy density, which is independent of the element size.

6. SUMMARY

In the work the selected quasi-static failure criteria and methods of parameters identification are presented. The closed formulae how to compute the constitutive parameters of those criteria are shown. All failure criteria are presented in meridian plane and in plane stress conditions to compare them. Energetic interpretation is also presented for selected failure criteria according to Burzyński concept. The concrete damage plasticity model is discussed together with parameters identification procedure and their interpretation. The reliable numerical results for asymmetric four points bending notched concrete beam are presented. Reliability of the results was confirmed by comparison with the known laboratory tests.

7. AKNOWLEDGEMENTS

The support of Ministry of Science and Higher Education under the grant N519 419435 is highly acknowledged.

REFERENCES

1. A. J. ABBO, S. W. SLOAN, *A smooth hyperbolic approximation to the mohr-coulomb yield criterion*, Computers and Structures, 427-441, 1995.
2. B. BRESLER, K. PISTER, *Strength of Concrete under Combined Stresses*, J. Am. Conc. Inst., **55**, 321-345, 1958.
3. W. T. BURZYŃSKI, *Studium nad hipotezami wytężenia*, Akademia nauk technicznych, Lwów: Academy of Technical Sciences, 1928.
4. A. C. T. CHEN, W.F. CHEN, *Constitutive relation for concrete*, J. Engng. Mech. Div., 465-481, 1975.
5. W. F. CHEN, *Plasticity in reinforced concrete*, NYC: McGraw-Hill Book Company, 1982.
6. D. C. DRUCKER, *A definition of stable inealastic materials*, J.Appl.Mech., 101-106, 1959.
7. W. DRUGAN, J. WILLIS, *A micromechanics-based nonlocal constitutive equation and estimates of representative volume element size for elastic composites*, J. Mech. Phys. Solids, **44**, 497-524, 1996.
8. A. GAWĘCKI, *Mechanika materiałów i konstrukcji prętowych*, Poznań: Politechnika Poznańska, 1998.
9. M. GEERS, R. DE BORST, R. PEERLINGS, *Damage and crack modeling in single-edge and double-edge notched concrete beams*, Engineering Fracture Mechanics, **65**, 247-261, 2000.
10. M. GEERS, R. DE BORST, W. BREKELMANS, R. PEERLINGS, *Strain-based transient-gradient damage model for failure analyses*, Computer Methods in Applied Mechanics and Engineering, 160(1/2), 133-154, 1998.

11. A. HILLEBORG, M. MODEER, P. PETERSSON, *Analysis of crack formation and crack growth in concrete by means of fracture mechanics and finite elements*, Cement and Concrete Research , **6**, 773-782, 1976.
12. T. JANKOWIAK, *Failure criteria for concrete under quasi-static and dynamic loadings* [in Polish], Poznań: Politechnika Poznańska, 2010.
13. T. JANKOWIAK, T. ŁODYGOWSKI, *Identification of parameters of concrete damage plasticity constitutive model*, Foundations of Civil and Environmental Engineering (6), 53-69, 2005.
14. L. KACHANOW, *O vremeni razrušenija v usloviach polzučesti*, Izv. Ak. Nauk CCCP, Otd. Techn. Nauk, 8, 26-31, 1958.
15. M. KLISINSKI, Z. MRÓZ, *Opis niesprezystych deformacji i uszkodzenia betonu*, Poznań: Rozprawy – Politechnika Poznańska, 1988.
16. H. KUPFER, H. K. HILSDO, H. RUSCH, *Behavior of concrete under biaxial stresses*, ACI Journal, 656-666, 1969.
17. J. LUBLINER, J. OLIVER, S. OLLER, E. OÑATE, *A Plastic-Damage Model for Concrete*, International Journal of Solids and Structures, **25**, 3, 229–326, 1989.
18. Z. MRÓZ, *Inelasticity and Non-linearity in Structural Concrete*, Waterloo: University Waterloo Press, 47-72, 1972.
19. A. NEVILLE, *Własciwosci betonu*, Kraków: Polski Cement, 2000.
20. R. B. PĘCHERSKI, *Burzyński yeld condition vis-A-vis the related studies reported in the literature*, Engineering Transactions , **56**, 4, 311-324, 2008.
21. S. PIETRUSZCZAK, Z. MRÓZ, *Finite element analysis of deformation of strain softening materials*, International Journal for Numerical Methods in Engineering, 327-334, 1981.
22. J. PODGÓRSKI, *Limit state condition and the dissipation function for isotropic materials*, Arch. Mech , **36**, 3, 323-342, 1984.
23. W. PRAGER, *Soil Mechanics and Plastic Analysis or Limit Design*, Q. Appl. Math., **10**, 2, 157-165, 1952.
24. E. SCHLANGEN, *Experimental and numerical analysis of fracture processes in concrete*, Delf: Delft University of Technology, 1993.
25. S. R. SWANSON, S. J. GREEN, *Static constitutive relations for concrete*, Kirtland Air Force Base: U.S.Air Force Weapon Laboratory, 1973.
26. M. SZUMIGAŁA, *Zespolone stalowo-betonowe konstrukcje szkieletowe pod obciążeniem doraźnym*, Poznań: Wydawnictwo Politechniki Poznańskiej, 2007.
27. R. VON MISES, *Mechanik der Festen Korper im plastisch deformablen Zustand*, Nachr. Math. Phys., I, 582-592, 1913.
28. K. WILLAM, W. WARNKE, *Constitutive Models for the Triaxial Behavior of Concrete*, Int. Assoc. Bridge Struct. Eng. Proc., **19**, 1-30, 1975.

QUASI-STATYCZNE KRYTERIA ZNISZCZENIA BETONU

Streszczenie

W pracy prezentuje się zachowanie betonu przy obciążeniach quasi-statycznych przy jednoosiowym ściskaniu i rozciąganiu oraz w płaskim stanie naprężenia. Dyskutowane są kryteria zniszczenia betonu oraz metody identyfikacji parametrów konstytutywnych. Istotnym elementem jest również energetyczna interpretacja omawianych kryteriów. Zawarto przykład numeryczny wykorzystujący model materiału betonu

plastycznego ze zniszczeniem, który dowodzi prawdziwości opisu konstytutywnego na podstawie wyników eksperymentalnych.

Remarks on the paper should be sent to the Editorial Office no later than September 30, 2010

Received January 05, 2010
revised version
June 15, 2010